Journal of Alloys and Compounds 404–406 (2005) 360–364

www.elsevier.com/locate/jallcom

Dynamics of positive muons in CaB_6

F.N. Gygax*, A. Schenck

Institute for Particle Physics of ETH Zurich, CH-5232 Villigen PSI, Switzerland

Received 29 July 2004; accepted 9 December 2004
Available online 14 July 2005

Abstract

We report on a muon spin relaxation and rotation (μSR) study in cubic $Ca_{0.995}La_{0.005}B_6$. The oriented sample has practically the lattice parameters of CaB_6 – space group $Pm3m$. A μSR investigation of CeB_6, isostructural with CaB_6 and with nearly the same lattice constants, has shown that the implanted μ^+ are located at the crystallographic d site and are immobile up to at least 200 K. Surprisingly, this is different for the μ^+ in CaB_6: they are at the interstitial 8 g site, and already for the lowest temperature range of the study, between 1.8 and ∼7 K, an apparently constant muon-spin relaxation of dynamical origin is present. This relaxation can only be explained by a mobile μ^+, e.g., by quantum diffusion, implying a hopping rate of $\approx 2 \times 10^5\,s^{-1}$. Between ∼7 and ∼70 K one observes an intermediate regime with slowly increasing mobility. True long range μ^+ diffusion appears to set in above ∼70 K. This picture describes in a consistent way a comprehensive set of zero-field, longitudinal-field and transverse-field μSR measurements performed for sample temperatures between 1.8 and 300 K.

Keywords: Hexaborides; Muon diffusion; Muon site; μSR

1. Introduction

Originally we had started a muon spin relaxation and rotation (μSR) study in lanthanum doped CaB_6 to understand the mysterious ultra-weak ferromagnetism claimed in this system [1]. Meanwhile it was demonstrated that this was not an intrinsic phenomenon but due to iron impurities near the surface [2]. We were, however, surprised to find that in $Ca_{0.995}La_{0.005}B_6$ the μ^+ polarization shows a relaxation of dynamical origin even below 2 K, an unexpected behavior, certainly not connected to a possible sample contamination. We present here our observations.

The host material of the sample is the divalent alkaline-earth hexaboride CaB_6. Its crystal structure – space group $Pm3m$ – can be thought of as a simple cubic ScCl-type arrangement of B_6-octahedra and metal ions. The lattice parameters are practically unchanged for $Ca_{0.995}La_{0.005}B_6$.

The $Ca_{0.995}La_{0.005}B_6$ sample consisted of several small oriented single crystals, thickness ∼0.5 mm, total area ∼5 mm × 5 mm. It was fixed on a Mylar tape suspended in the cryostat on a fork-like holder which did not overlap with the μ^+-beam spot. The initial μ^+ polarization $\boldsymbol{P}_\mu(t=0)$ or the applied magnetic field $\boldsymbol{H}_{ext}$ were parallel to the [0 0 1] axis.

The experiment was realized at the GPS and Dolly instruments of the Paul Scherrer Institut (PSI). Various zero-field (ZF), transverse-field (TF) and longitudinal-field (LF) μSR measurements have been performed for sample temperatures between 1.8 and 300 K.

2. ZF measurements

The μSR signal $P_\mu^{ZF}(t)$ cannot be correctly described, even at the lowest T of 1.8 K, with a relaxation function considering only distributions of *static* fields at the μ^+ location. On the other hand a *dynamic* Kubo-Toyabe (dKT) relaxation function [3] fits well all ZF-μSR spectra, taken between 1.8 and 300 K. The dKT relaxation function is characterized by Δ^2, the second moment of the field distribution along a spatial direction, and ν, the fluctuation rate of the local fields. We define the correlation time τ_c as $\tau_c = 1/\nu$. Fig. 1 shows the obtained temperature dependence of τ_c. The dKT fits of the spectra yield for the second parameter a constant value

* Corresponding author. Tel.: +41 56 310 32 25; fax: +41 56 310 43 62.
E-mail address: fredy.gygax@psi.ch (F.N. Gygax).

0925-8388/$ – see front matter
doi:10.1016/j.jallcom.2004.12.161

Table 1
Parameters used to describe $\tau_c(T)$ with Eqs. (1) and (2)

Data fitted (line Fig. 1)	τ_{max} (μs)	$\tau_{\infty,1}$ (μs)	$E_{a,1}/k_B$ (K)	$\tau_{\infty,2}$ (μs)	$E_{a,2}/k_B$ (K)
ZF (solid)	4.72 (25)	1.93 (13)	22 (3)	0.0115 (15)	475 (16)
LF (dashed)	4.72	1.93	22	0.0003	800

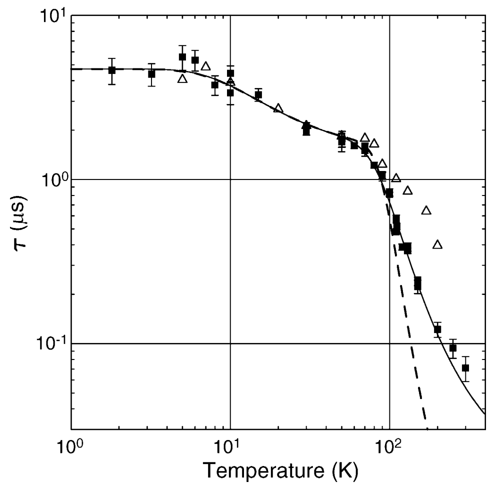

Fig. 1. Temperature dependence of the correlation times τ_c (squares), dKT fits of ZF data, and τ_A (triangles), Abragam-fits of TF data. The solid line is a fit of the ZF τ_c with Eqs. (1) and (2), the dashed line a deviation needed to explain the LF data.

$\gamma_\mu \Delta = 0.55\ \mu s^{-1}$ for $T \lesssim 70$ K. (γ_μ, the μ^+ gyromagnetic ratio, amounts to $\gamma_\mu = 85.16 \times 10^6$ rad s^{-1} kOe^{-1}.) Above 70 K it is not possible to obtain τ_c and Δ independently. For the τ_c values shown in Fig. 1 above 70 K a persisting constant value $\gamma_\mu \Delta = 0.55\ \mu s^{-1}$ was assumed. The behavior of $\tau_c(T)$ is perfectly described assuming that the rate $\nu(T)$ is the sum of three rates, each one dominant in a particular T interval:

$$\frac{1}{\tau_c(T)} = \frac{1}{\tau_{max}} + \frac{1}{\tau_1(T)} + \frac{1}{\tau_2(T)}. \qquad (1)$$

The constant τ_{max} corresponds to the largest but finite observed correlation time, at low T, and $\tau_i(T)$, $i = 1$ and 2, are each given by Arrhenius expressions of the form

$$\tau_i = \tau_{\infty,i} \exp\left(\frac{E_{a,i}}{k_B T}\right). \qquad (2)$$

The parameters, yielding the solid line in Fig. 1, are listed in Table 1.

3. TF measurements

TF measurements have been performed with a field $H_{ext} = 6$ kOe for various temperatures between 5 and 200 K. The μ-spin rotation spectra can be fitted with the commonly called “Abragam relaxation formula” [4], which among other parameters involves M_2, the second moment of the field distribution along $\boldsymbol{H}_{ext}$, and a correlation time τ_A characterizing the field fluctuation. Again, except at the lowest temperature, the fits do not yield M_2 and τ_A independently. Fixing the second moment such as $\gamma_\mu M_2^{-1/2} = 0.36\ \mu s^{-1}$, one obtains the τ_A values also shown in Fig. 1 (triangles). The τ_A are compatible with the ZF τ_c below 70 K, but deviate above this temperature to larger values.

4. LF measurements

The spin lattice relaxation rate λ_1 can be studied with ZF or LF measurements. In ZF $P_\mu^{ZF}(t)$ may also be affected by static field distributions, and it may be difficult to distinguish static and dynamic features. In longitudinal fields one can decouple the μ^+ spin from static fields and $P_\mu^{LF}(t)$ will only reflect λ_1. Therefore, we have performed LF scans [i.e., $\boldsymbol{H}_{ext} \| \boldsymbol{P}_\mu(t = 0)$] at different temperatures and T scans at different H_{ext}. For $H_{ext} \geq 25$ Oe the decoupling is effective and $P_\mu^{LF}(t) \propto \exp(-\lambda_{LF} t)$. Fig. 2 displays $\lambda_{LF}(H_{ext})$ and Fig. 3 $\lambda_{LF}(T)$ for part of the LF-data sets. Fig. 2 reveals a peak of λ_{LF} at ~73 Oe, a feature which tends to disappear for $T > 100$ K. We attribute this peak to quadrupolar level crossing (QLC) arising from the degeneracy of the μ^+-Zeeman splitting and ^{11}B quadrupolar splitting at a certain H_{ext} [5]. The quadrupolar splitting is of the order of 0.60 MHz for $Ca_{0.995}La_{0.005}B_6$ [6], while the $\lambda_{LF}(H_{ext})$ peak position corresponds to a frequency of $(\gamma_\mu/2\pi)H_{ext} \cong 0.99$ MHz. The larger value points to a modified electric field gradient (EFG) at the μ^+ nearest ^{11}B neighbors due to the presence of the μ^+. Reference [5] indicates that the QLC signal assumes a Gaussian shape as a function of H_{ext}. A second contribution to λ_{LF}, reflecting the spin-lattice relaxation and described by the Redfield theory [7], is also present. Its clear signature is visible in the $\lambda_{LF}(T)$ sequence – Fig. 3 – as a peak with decreasing height and weakly increasing T position for increasing H_{ext}. Hence we write

$$\lambda_{LF}(H_{ext}, T) = \frac{C}{\Delta B} \exp\left\{\frac{-(H_{ext} - B_0)^2}{\Delta B^2}\right\} + \frac{A^2 \tau_c}{1 + \omega^2 \tau_c^2} + \lambda_0, \qquad (3)$$

where C, ΔB and B_0 are, respectively, amplitude, width and position of the QLC signal, A^2 is the square of the amplitude of fluctuating field components at the μ^+, $\omega = \gamma_\mu H_{ext}$, and λ_0 a field and/or temperature independent term.

We try now to describe $\lambda_{LF}(H_{ext})$ and $\lambda_{LF}(T)$ with Eq. (3). This can only be achieved by allowing a temperature dependence for the parameters C, ΔB, B_0 and A^2. Yet, retaining for $\tau_c(T)$ the ZF behavior with the original parameters of

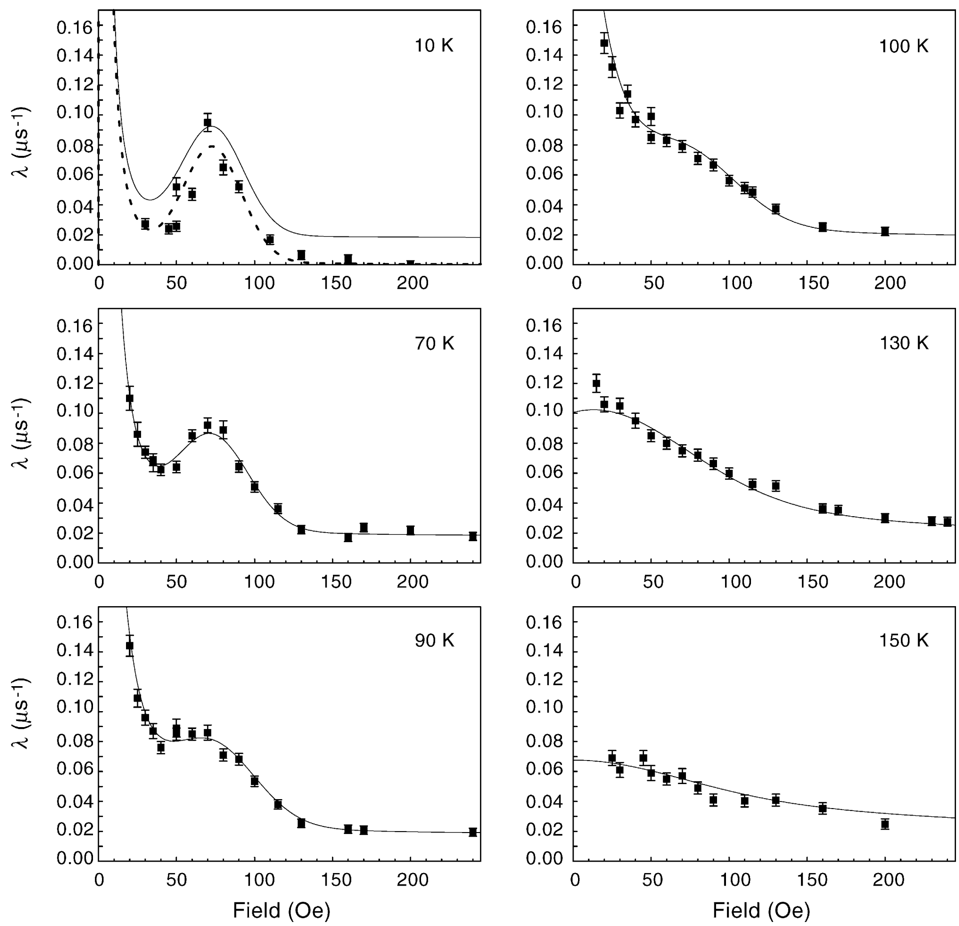

Fig. 2. Field dependence of the LF spin-lattice relaxation rate λ_{LF} for selected temperatures. The solid lines are calculations with a unique set of parameters (dotted line for $T = 10$ K from a T-dependent λ_0, see Fig. 4)

Table 1, a consistent solution cannot be found: the position of the "Redfield peak" (Fig. 3) shifts up too fast with increasing field. However, using a different set of optimized parameters for $\tau_c(T)$ – presented in Table 1, second row – leading to the dashed line in Fig. 1, a consistent fit of the data (Figs. 2 and 3) can be achieved (solid lines). This fit is obtained with fixed $\lambda_0 = 0.018\ \mu s^{-1}$, $C = 0.0002\ \mu s^{-1}$, $A^2 = 0.47\ \mu s^{-2}$, and the T dependent B_0 and ΔB shown in Fig. 4.

5. Discussion

A μSR study of CeB_6, which is isostructural with CaB_6 and has nearly the same lattice constant, has shown that the implanted μ^+ are located at the crystallographic 3d sites (on the cube edges, in the middle between two Ca ions) and are immobile up to at least 200 K [8]. For this location in CaB_6 one calculates for our ZF case a field distribution arising from the uncorrelated ^{11}B nuclear dipole moments corresponding to a value between $\gamma_\mu \Delta^{vV} = 0.345\ \mu s^{-1}$ [van Vleck (vV) limit] and $\gamma_\mu \Delta^{rq} = 0.308\ \mu s^{-1}$ [radial quadrupolar (rq) limit]. For the TF case one calculates as limits $\gamma_\mu (M_2^{vV})^{-1/2} = 0.258\ \mu s^{-1}$ and $\gamma_\mu (M_2^{rq})^{-1/2} = 0.308\ \mu s^{-1}$. Obviously, the values for $\gamma_\mu \Delta$ and $\gamma_\mu M_2^{-1/2}$ deduced from our ZF and TF measurements are not compatible with these calculations for the 3d site, and thus indicate that in CaB_6 the μ^+ must reside at a different location.

A suitable interstitial μ^+ location can be found: the 8g site, generic co-ordinates (x, x, x), with, e.g. $x = 0.23$ (between a Ca ion and the B_6-octahedron on the cube diagonal). We calculate the limits $\gamma_\mu \Delta^{vV} = 0.576\ \mu s^{-1}$, $\gamma_\mu \Delta^{rq} = 0.515\ \mu s^{-1}$, and $\gamma_\mu (M_2^{vV})^{-1/2} = 0.286\ \mu s^{-1}$, $\gamma_\mu (M_2^{rq})^{-1/2} = 0.515\ \mu s^{-1}$, which bracket the measured values. Furthermore, considering the crude modeling of the LF data, which yields for the fluctuating field amplitude $B_\sim = A/\gamma_\mu = 8.1$ G, one has good agreement with the value calculated for the 8g site: $B_\sim = 8.8$ G. [The amplitude of fluctuating field components seen in ZF by a randomly hopping μ^+ is $B_\sim = (2\Delta^2)^{1/2}/\gamma_\mu$.]

The exact calculation of Δ^2 and M_2 for the various μ^+ sites is not feasible. As seen, the EFG is modified by the μ^+, its strength and orientation is difficult to estimate for all ^{11}B neighbors of the muon. In addition, there is usually a small, a priori unknown lattice relaxation around the μ^+. Hence, the quoted limits serve as rough estimates.

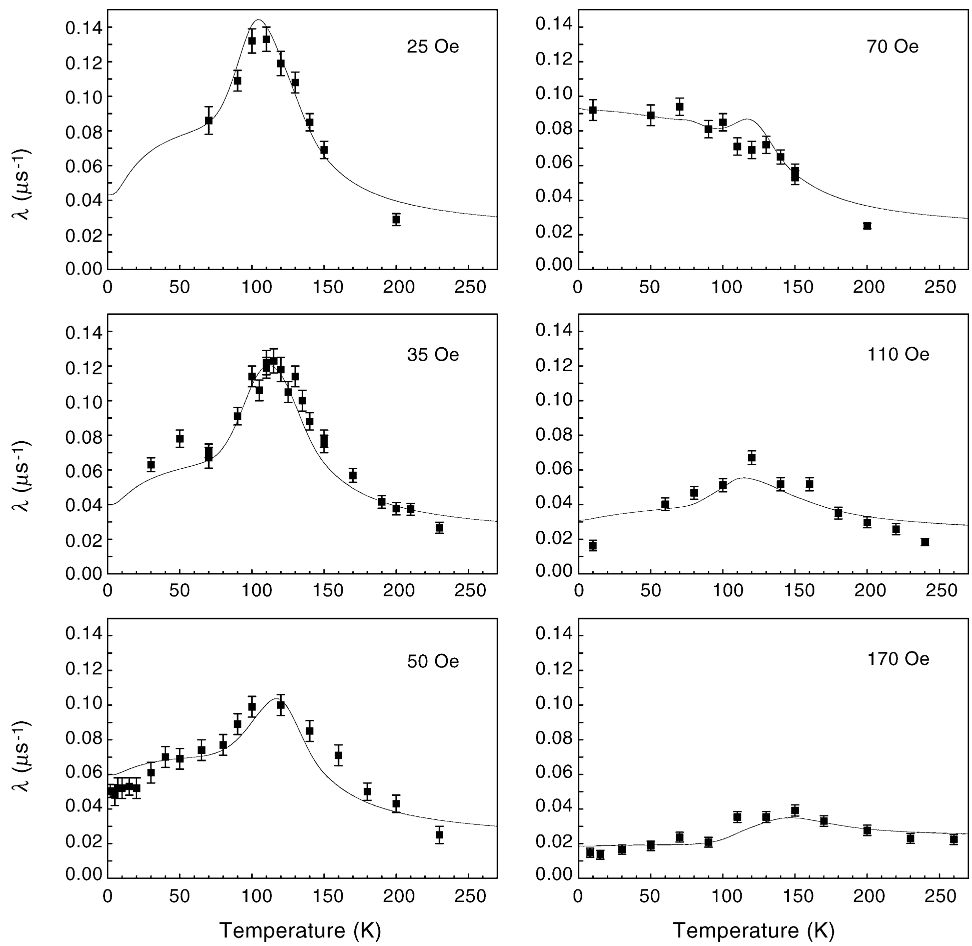

Fig. 3. Temperature dependence of the LF spin-lattice relaxation rate λ_{LF} for selected fields. The solid lines are calculations with the same set of parameters as in Fig. 2.

The temperature dependence of τ_c (Fig. 1) implies the existence of two, possibly three T regimes: the high-T regime above the kink at ∼70 K, and below the low-T domain. The latter is apparently split, above ∼7 K one has an intermediate regime with varying relaxation, below ∼7 K a domain of constant relaxation. As seen, to fit the LF data it was necessary to modify $\tau_c(T)$, retaining a faster drop of the correlation time

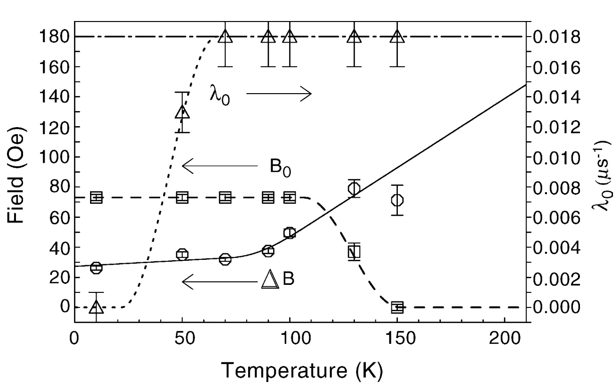

Fig. 4. Temperature dependence of the QLC parameters B_0 (dashed line) and ΔB (solid line). The data points are given by fits of $\lambda_{LF}(H_{ext})$ with Eq. 3. [As alternative to a constant λ_0 (dash-dotted line) an improvement with λ_0 tending to 0 at low T is also indicated].

with rising T in the high temperature region. The LF data give a more direct estimate of τ_c, and the proposed modification is certainly closer to reality. This argument is reinforced by tests showing that in this T region the results of dKT fits were very sensitive to parameters like Δ^2, μ^+-decay asymmetries, etc. (Similar arguments explain the deviation of the TF data from the effective τ_c above 70 K; in this region the τ range renders a simple Abragam fit of $P_\mu^{TF}(t)$ with fixed M_2 crude and unstable.) From NMR measurements [6] it is known that the ^{11}B-spin relaxation rates are very low and can be considered as static within the μSR time window. Dynamics will however appear if the μ^+ moves through the 8g sites. The low-temperature relaxation seems to reflect quantum diffusion of the μ^+, implying a hopping rate of $\approx 2 \times 10^5\,\mathrm{s}^{-1}$ between 1.8 and 6 K. True long range μ^+ diffusion appears to set in above ∼70 K.

Acknowledgements

We thank the Laboratory for Muon-Spin Spectroscopy (LMU) and the PSI for providing excellent measuring conditions. We are grateful to H.R. Ott (ETH Zurich) and Z. Fisk (Florida State University) for providing the sample.

References

[1] D.P. Young, et al., Nature 397 (1999) 412.
[2] T. Mori, S. Otani, Solid State Commun. 123 (2002) 287.
[3] A. Schenck, F.N. Gygax. In: K.H.J. Buschow (Ed.), Handbook of Magnetic Materials, vol. 9, Elsevier, Amsterdam, 1995, p. 57.
[4] A. Abragam, The principles of nuclear magnetism, Clarendon Press, Oxford, 1970.
[5] S.R. Kreitzman, Hyperfine Interact 31 (1986) 13.
[6] J.L. Gavilano, et al., Phys. Rev. B 36 (2001) 140410–140411.
[7] C.P. Slichter, Principles of Magnetic Resonance, Springer, Berlin, 1990.
[8] A. Schenck, F.N. Gygax, S. Kunii, Phys. Rev. Lett. 89 (2002) 037201.